Hindawi
Advances in Materials Science and Engineering
Volume 2020, Article ID 2781928, 7 pages
https://doi.org/10.1155/2020/2781928

Research Article

Experimental Study on the Effect of Offset Notch on Fracture Properties of Rock under Three-Point Bending Beam

Qifeng Guo,[1,2] **Xinghui Wu**,[1,2] **Meifeng Cai**,[1,2] **and Shengjun Miao**[1,2]

[1]*School of Civil and Resource Engineering, University of Science and Technology Beijing, Beijing 100083, China*
[2]*Beijing Key Laboratory of Urban Underground Space Engineering, School of Civil and Resource Engineering, University of Science and Technology Beijing, Beijing 100083, China*

Correspondence should be addressed to Qifeng Guo; guoqifeng@ustb.edu.cn

Received 6 November 2019; Revised 24 December 2019; Accepted 13 January 2020; Published 8 February 2020

Academic Editor: Paulo Reis

To investigate the effects of offset notch on the fracture properties of rock beam under bending load, granite beam specimens with "one single offset notch" and "central and offset double notches" are made. A series of three-point bending beam tests on the specimens are carried out by controlling the displacement rate of central notch. The whole load-displacement (P-CMOD) curves are obtained. Experimental results show that the larger the distance between the offset notch and beam central is, the larger are the peak load and nominal strength of the specimen. The peak load and nominal strength for the "central and offset double notches" specimens are both larger than those for the "single central notch" specimen. A fracture model considering the effect of offset notch is developed, and the relationship between the offset notch parameter, tensile strength, and fracture toughness is established.

1. Introduction

Rock fracture is one of the most important topics on rock mechanics, which dominates rock projects failure such as dam instability, landslide, and tunnel collapse [1–3]. The macrofailure of rock mass is caused by microcracks initiation, coalescence, and propagation. The fracture properties of rock are attracting more attention for understanding the fracture behaviors of different rock types under different external loads.

There are three typical experimental methods for obtaining the fracture parameters for rock: the Brazilian disc test, direct tensile test, and three-point bending test [1, 4–6]. The Brazilian disc test is the most popular method for measuring the rock tensile strength because the disc specimen is easy to make [1]. However, whether the strength from the disc test is the true tensile strength is unknown. Also, it is hard to know the postpeak behavior of rock through the Brazilian disc test. The direct tensile test is an ideal method for obtaining the whole stress-displacement curve for rock [4, 5]. However, it is difficult to control the crack mouth opening when holding the top and bottom of the rock specimen for tension. Through the three-point beam beading test, stable crack propagations in quasibrittle materials (e.g., rock and concrete) can be achieved by controlling the crack mouth opening displacement [6, 7]. Therefore, the three-point bending beam test has been an effective method for obtaining rock fracture properties through the whole load-crack mouth opening displacement (P-CMOD) curve [6–9].

Fakhimi et al. [7] studied the development of fracture process zone of rock by the three-point beam test. Guo et al. [8] investigated the fracture process of rock by acoustic emission monitoring by the three-point beam test and found that the events of acoustic emission exhibited four stages such as gradually increasing, fastly increasing, suddenly increasing, and gradually decreasing with the development of load. Wang et al. [9] investigated the effect of temperature on granite mechanical behavior by adapting the three-point bending test and found that the elastic modulus of granite decreased with increasing temperature. Huang et al. [10] employed a numerical method to simulate the dynamic fracture of rock under the three-point bending test and found that the crack pattern of the rock beam was changed

by the notch location. Xi et al. [11–13] modelled mesoscale mixed-mode cracking of concrete and found that corrosion-induced concrete cracking is dominated by tensile fracture. Liao et al. [14] tried to eliminate the effect of beam gravity in the bending test by applying horizontal forces to the beam and obtained the fracture toughness of rock. Cheng et al. [15] modelled the cracking of asphalt concrete with offset notches by the three-point bending test and found that the larger the distance between the offset notch and beam central span, the larger the maximum load is. Wang et al. [16] formulated the relationship between the deflection and CMOD and employed a numerical method to parametrize the formulation. [17] developed a numerical method to investigate the effect of particle size on rock fracture under the three-point bending test.

For geotechnical projects, the natural fractures in rock mass significantly affect the fracture behavior of the rock structure, and the external load direction is more likely not in a straight line with the pre-notch. However, most existing research studies on the three-point bending test were carried out on single notch beam, and the effect of initial cracks on rock fracture was rarely evaluated [11–19]. The knowledge on the effect of offset notch on fracture properties of rock beam is limited. This paper proposed a three-point bending beam test method for rock beams with offset notches at different locations. The rock beam specimens are made as two types, i.e., one single offset notch" and "central and offset double notches." The whole P-CMOD curves from 18 notched granite samples are obtained. Furthermore, the effects of offset notches on maximum load are analyzed. Finally, the relationships between the tensile strength and fracture toughness and offset notch parameter are formulated.

2. Experimental Program

Granite specimens are firstly made as beams of the dimensions 145 mm (length) × 50 mm (height) × 18 mm (width). As shown in Figure 1, the span length is 127 mm and the notch height is 10 mm. There are two types of the notched granite beams: specimens with one single offset notch (Figure 1(a)) and specimens with central and offset double notches (Figure 1(b)). The distance between the offset notch and beam center at the bottom is named as offset distance C. Furthermore, the offset rate describing the offset degree for a beam is expressed as follows:

$$N = \frac{2C}{L} \times 100\%, \tag{1}$$

where L is the length of the beam.

The specimen number "B10%-1" denotes the first beam of one single offset notch with $N = 10\%$. The specimen number "BC30%-1" denotes the first beam of central and offset double notches with $N = 30\%$. A closed loop servo-controlled testing machine MTS810 is employed for loading the specimen. A clip gauge was mounted on the bottom of the beam to measure the crack mouth opening displacement (CMOD). The tests are performed under the CMOD control mode with a rate of 0.5 μm/s. More details on the three-point beam test can be found on the standard ASTM C78 [20] and other publications [7, 21].

3. Experimental Results

3.1. Specimens with One Single Offset Notch. Eighteen specimens with one single offset notch were divided into six groups whose offset rates were 0%, 10%, 20%, 30%, 40%, and 50%, respectively. There are three specimens for each offset rate. The peak loads for the specimens with one single offset notch are listed in Table 1.

Figure 2 shows the P-CMOD curves obtained from experiments. The load-displacement development can be classified as three stages. At the first stage, the load linearly increases with increasing CMOD, which can be regarded as the linear elastic stage. The difference of the linear elastic stage in the figures is mainly caused by the different porosities of the samples. Also, the test for B40%-3 was failed, which was excluded in the further analysis. Furthermore, with the development of displacement, the load keeps increasing but with a smaller slope, which can be seen as the nonelastic stage. Finally, after reaching the peak load, the load gradually decreases, which is the post-peak stage. The average peak loads for specimens with offset rates 0%, 10%, 20%, 30%, 40%, and 50% are 2.57, 2.87, 3.12, 3.51, 4.14, and 4.20, respectively. The larger the offset distance is, the larger the peak load is. The effect of the offset notch on the peak load is almost the same when the offset rate is larger than 40%. It is probably because the fracture mode has been changed from mode I to mixed mode with increasing offset rate.

3.2. Specimens with Central and Offset Double Notches. Three specimens with central and offset double notches were made, and the offset rates are 30%, 40%, and 50%, respectively. The number and peak load of the specimens are listed in Table 2. It can be seen that the larger the offset distance is, the larger the peak load is. Figure 3 shows the P-CMOD curves of the specimens with central and offset double notches. It can be found that the load gradually increases with the displacement. After the peak point, the load decreases in a slower rate than that for specimen with one single notch. The larger the offset rate is, the larger the crack mouth opening displacement to the peak load is. The peak loads for the doubled notched specimens BC30% (2.71 kN) and BC40% (2.92 kN) are smaller than those for the single notched specimens B30% (3.44 kN) and B40% (4.14 kN) while larger than that for the single notched specimen B0% (2.5722 kN).

4. Analysis and Discussion

The relationship between nominal strength of the specimen and the peak load can be calculated by the following equation:

$$\sigma_n = \frac{3\mathrm{SP}_{\max}}{2T\left(W - a_0\right)^2}, \tag{2}$$

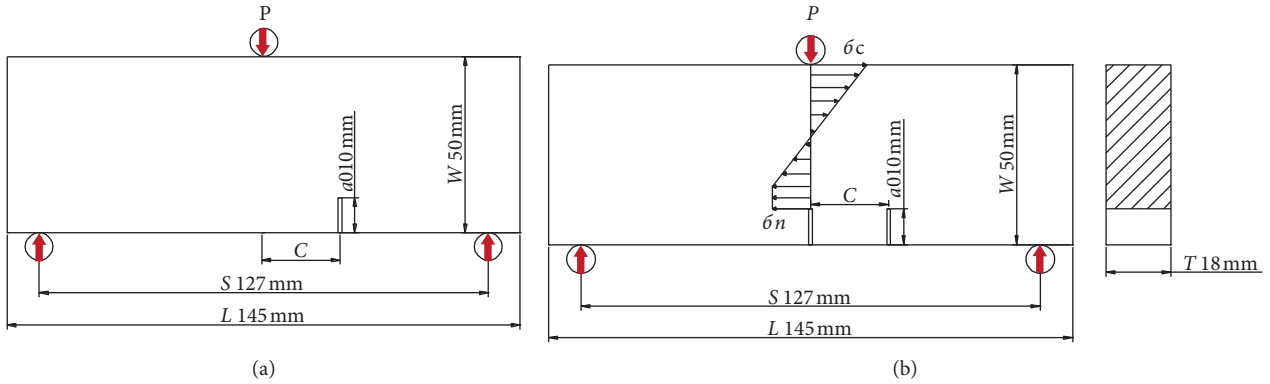

Figure 1: Specimens design and experimental setup. (a) Specimens with one single offset notch. (b) Specimens with central and offset double notches.

Table 1: Peak loads for the specimens with one single offset notch.

Specimens	Offset distance (mm)	Peak load (kN)	Average peak load (kN)
B0%-1		2.5086	
B0%-2	0	2.2371	2.57
B0%-3		2.9709	
B10%-1		3.2326	
B10%-2	7.25	2.6326	2.87
B10%-3		2.7414	
B20%-1		2.9811	
B20%-2	14.5	3.1984	3.12
B20%-3		3.1866	
B30%-1		3.5656	
B30%-2	21.75	3.4409	3.51
B30%-3		3.5373	
B40%-1		4.1714	
B40%-2	29.00	4.1164	4.14
B40%-3		N/A	
B50%-1		4.1903	
B50%-2	36.25	4.1959	4.20
B50%-3		4.2000	

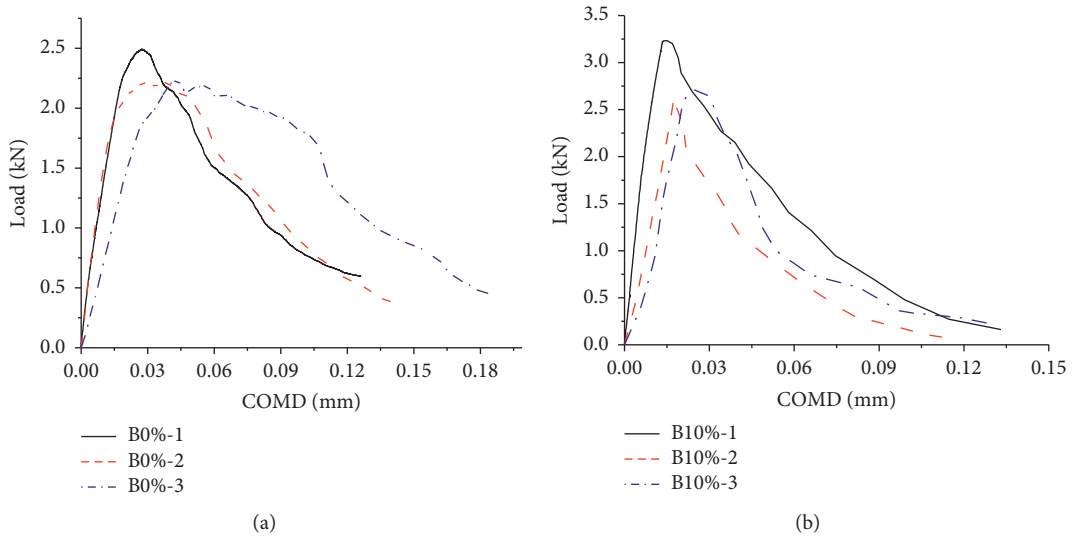

Figure 2: Continued.

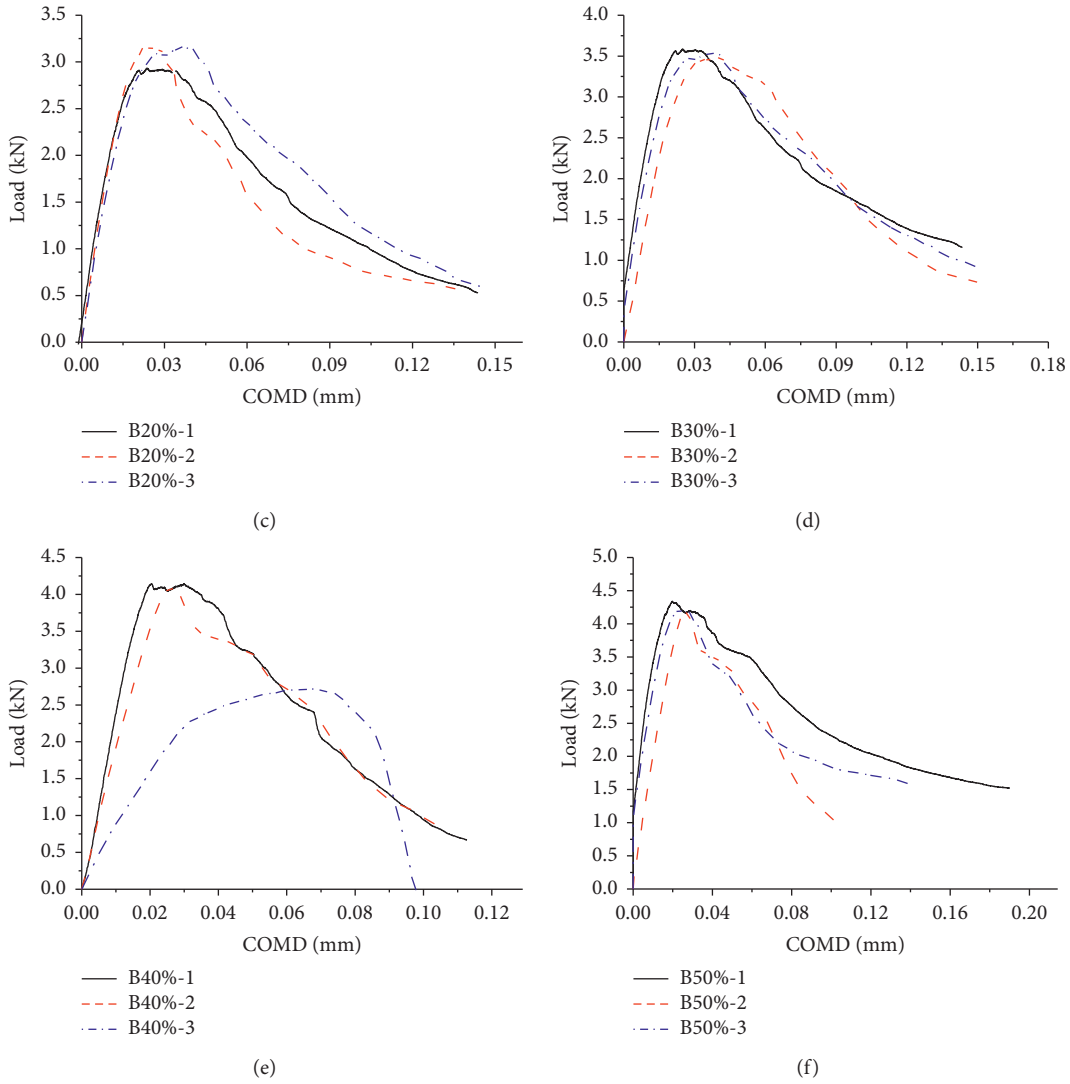

Figure 2: P-CMOD curves for the specimens with one single offset notch. (a) Offset rates 0%. (b) Offset rates 10%. (c) Offset rates 20%. (d) Offset rates 30%. (e) Offset rates 40%. (f) Offset rates 50%.

Table 2: Peak loads for the specimens with central and offset double notches.

Specimens (%)	Offset distance (mm)	Peak load (kN)
BC30	21.75	2.71
BC35	25.38	2.82
BC40	29.00	2.92

where σ_n is the nominal strength [22]; S is the span length; T is the beam width; W is the beam height; P_{max} is the peak load; and a_0 is the height of the notch.

By substituting the average peak loads from experiments on the specimens with one single offset notch into equation (2), the nominal strengths of the specimens can be obtained. Figure 4 illustrates the effect of the offset rate on the nominal strength of specimens. It can be found that the larger the offset rate is, the larger the nominal strength is.

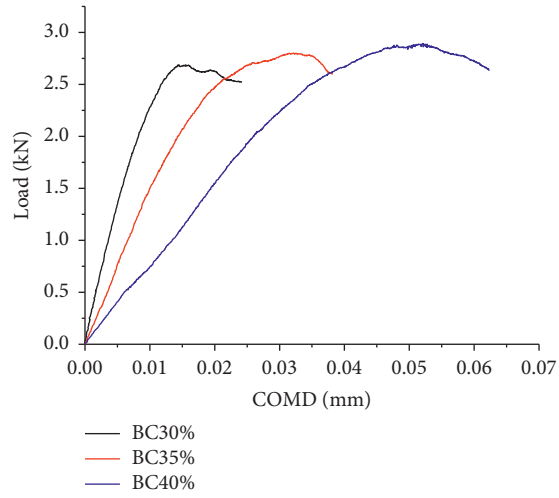

Figure 3: P-CMOD curves for the specimens with central and offset double notches.

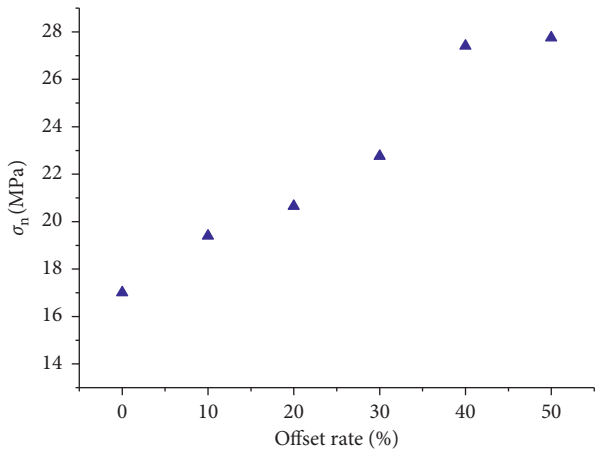

Figure 4: Effect of the offset rate on the nominal strength.

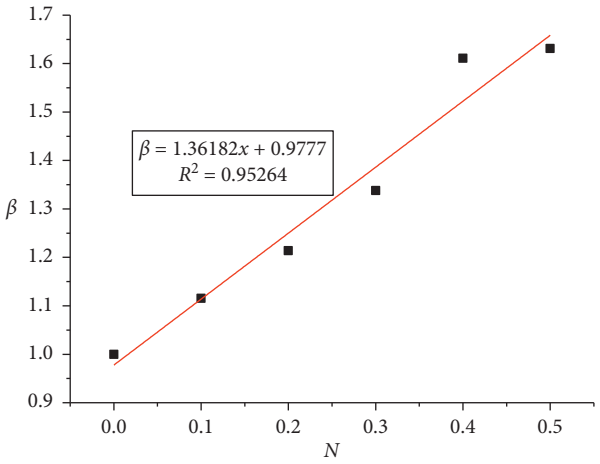

Figure 5: Calculation of the offset parameters.

However, the tensile strength and fracture toughness of the specimen are regarded as the material constant properties, which will not change with the offset notch [22–24]. Therefore, we proposed a fracture model to calculate the tensile strength and fracture toughness for the offset notched rock specimens [25]. The nominal strength can be expressed as a function of the tensile strength and fracture toughness:

$$\sigma_n = \frac{f_t}{\sqrt{1 + (a_e/a_{\infty}^*)}}, \qquad a_{\infty}^* = 0.25 \cdot \left(\frac{K_{IC}}{f_t}\right)^2, \tag{3}$$

where f_t and K_{IC} are the tensile strength and fracture toughness, respectively; a_{∞}^* is the length of the fracture process zone; and a_e is the equivalent crack length used instead of the actual one, which can be expressed as follows:

$$a_e = \left(\frac{(1-\alpha)^2 \cdot Y(\alpha)}{1.12}\right) \cdot a_0, \tag{4}$$

where α is the ratio of the notch height to the specimen height and a_0 is the notch height. $Y(\alpha)$ is a geometric parameter formulated as follows:

$$Y(\alpha) = \frac{1.99 - \alpha \cdot (1-\alpha) \cdot (2.15 - 3.93 \cdot \alpha + 2.7\alpha^2)}{\sqrt{\pi} \cdot (1 + 2 \cdot \alpha) \cdot (1-\alpha)^{3/2}}, \quad \text{for } \alpha \le 1. \tag{5}$$

Furthermore, the relationship between the nominal strength and the tensile strength and fracture toughness can be described as follows [26]:

$$\frac{1}{{\sigma_n}^2} = \frac{1}{f_t^2} + \frac{1}{f_t^2 + a_{\infty}^*} \cdot a_e = \frac{1}{f_t^2} + \frac{4}{K_{IC}^2} \cdot a_e. \tag{6}$$

The abovementioned equation can be used to calculate the tensile strength and fracture toughness of the specimen with the single central notch ($N = 0\%$) [26–30]. The formula for calculating the nominal strength of the specimens with offset notches is the same as that of single notched specimens. Furthermore, we introduced a parameter β as the ratio of nominal strength of specimens with offset notches to those with single central to describe the effect of offset notch, which could be expressed as follows:

$$\beta = \frac{\sigma_{nN}}{\sigma_{no}}, \tag{7}$$

where σ_{no} is the nominal strength calculated by equation (2) for the specimen with central notch ($N = 0\%$); σ_{nN} is the nominal strength calculated by equation (2) for the specimen with offset notch (N is not equal to 0%).

Figure 5 shows the offset parameter development as a function of offset rate. It can be seen that the lager the offset rate is, the larger the offset parameter is. By fitting the curve by a linear function, the relationship between the offset parameter β and the offset rate N is formulated as follows.

$$\beta = 1.36182N + 0.9777. \tag{8}$$

Furthermore, $1/\sigma_n^2$ in equation (6) for using the nominal strength of the central notched specimen can be expressed as follows:

$$\frac{1}{\sigma_n^2} = \frac{1}{((1.36182\,(C/(L/2)) + 0.9777)\sigma_{n0})^2}. \tag{9}$$

The tensile strength and fracture toughness for the specimens with one single offset notch can be obtained by the following equation:

$$\frac{1}{((1.36182C/L/2 + 0.9777)\sigma_{n0})^2} = \frac{1}{f_t^2} + \frac{4}{K_{IC}^2} \cdot a_e. \tag{10}$$

5. Conclusions

In this paper, comprehensive experiments on granite specimens with "one single offset notch" and "central and offset double notches" were carried out. The whole P-CMOD curves for the specimens were obtained. Based on the

experimental results, the effects of the offset notch on tensile strength and fracture toughness of granite were analyzed and discussed. A fracture model for calculating the real tensile strength of a granite specimen with the offset notch was developed. It has been found that the larger the distance between the offset notch and the beam bottom central is, the larger the peak load is. The value of peak load for specimens with "central and offset double notches" is between that for specimens with "central single notch" and that for specimens with "single offset notch." The introduced offset parameter can be used to calculate the tensile strength and fracture toughness for the offset notched specimens.

Data Availability

The test data used to support the findings of this study are included within the article.

Conflicts of Interest

The authors declare that they have no conflicts of interest.

Acknowledgments

This work was supported by Fundamental Research Funds for the Central Universities (no. FRF-TP-18-015A3) and National Key R&D Program of China (no. 2018YFE0101100).

References

[1] R. Ulusay, *The ISRM Suggested Methods for Rock Characterization, Testing and Monitoring: 2007–2014*, Springer International Publishing, vol. 15, no. 1, Berlin, Germany, 2014.

[2] Z. P. Bazant and J. L. Le, "Review of classical statistical theory of structural strength and structural safety, and of statistics fundamentals," in *Probabilistic Mechanics of Quasibrittle Structures (Strength, Lifetime, and Size Effect)*, vol. 2, pp. 22–34, Cambridge University Press, Cambridge, UK, 2017.

[3] Q. B. Zhang and J. Zhao, "A review of dynamic experimental techniques and mechanical behaviour of rock materials," *Rock Mechanics and Rock Engineering*, vol. 47, no. 4, pp. 1411–1478, 2014.

[4] T. Kazerani, "Effect of micromechanical parameters of microstructure on compressive and tensile failure process of rock," *International Journal of Rock Mechanics and Mining Sciences*, vol. 64, no. 6, pp. 44–55, 2013.

[5] B. I. G. Barr, M. K. Lee, B. Barragán et al., "Round-robin analysis of the RILEM TC 162-TDF uni-axial tensile test: part 2," *Materials and Structures*, vol. 36, no. 4, pp. 275–280, 2003.

[6] B. I. G. Barr, M. K. Lee, E. J. de Place Hansen et al., "Round-robin analysis of the RILEM TC 162-TDF beam-bending test: part 1—test method evaluation," *Materials and Structures*, vol. 36, no. 9, pp. 609–620, 2003.

[7] A. Fakhimi, A. Tarokh, and J. F. Labuz, "Cohesionless crack at peak load in a quasi-brittle material," *Engineering Fracture Mechanics*, vol. 179, no. 5, pp. 272–277, 2017.

[8] Y. S. Guo, W. S. Zhu, S. C. Li, C. J. Lin, N. D. Wen, and L. Yang, "Acoustic emission properties of tensile fracture under different load patterns," *Geotechnical Mechanics*, vol. 27, no. S2, pp. 1055–1058, 2006.

[9] G. D. Wang, *Experimental Research on the Effects of Temperature and Viscoelastoplastic Analysis of Beishan Granite*, Xi'an University of Science and Technology, Xi'an, China, 2003.

[10] M. L. Huang, W. C. Zhu, and M. Z. Pang, "Numerical simulation of dynamic failure process of three-point bending beam with offset notch," *Chinese Journal of Rock Mechanics and Engineering*, vol. S1, pp. 3384–3389, 2007.

[11] X. Xi, S. Yang, C.-Q. Li, M. Cai, X. Hu, and Z. K. Shipton, "Meso-scale mixed-mode fracture modelling of reinforced concrete structures subjected to non-uniform corrosion," *Engineering Fracture Mechanics*, vol. 199, pp. 114–130, 2018.

[12] X. Xi, S. Yang, and C.-Q. Li, "A non-uniform corrosion model and meso-scale fracture modelling of concrete," *Cement and Concrete Research*, vol. 108, pp. 87–102, 2018.

[13] X. Xi and S. Yang, "Investigating the spatial development of corrosion of corner-located steel bar in concrete by X-ray computed tomography," *Construction and Building Materials*, vol. 221, pp. 177–189, 2019.

[14] P. W. Liao and H. M. Tang, "Experimental study on the fracture toughness K_{IC} of soil," *Journal of Chongqing Jiaotong University (Natural Science Edition)*, vol. 31, no. 4, pp. 788–791, 2012.

[15] Y. Cheng, X. Yang, and C. Zhang, "Numerical simulation for three-point bending fracture of asphalt mixture based on extended finite element method," *Chinese Journal of Solid Mechanics*, vol. 38, no. 3, pp. 281–286, 2017.

[16] Q. Y. Wang, H. N. Chen, H. G. Zhang, C. Liu, Y. B. Zhao, and X. Z. Huang, "Relationship of deflection and crack mouth opening displacement of concrete beams under the three-point bending," *Chinese Journal of Applied Mechanics*, vol. 34, no. 5, pp. 937–943, 2017.

[17] J. P. Zuo, H. P. Xie, Y. J. Liu, B. Hu, and J. F. Lu, "Investigation on fracture characteristics of sandstone after thermal effects through three-bending point experiment," *Chinese Journal of Solid Mechanics*, vol. 31, no. 2, pp. 119–126, 2010.

[18] Y. S. Wang and X. Z. Hu, "Determination of tensile strength and fracture toughness of granite using notched three-point-bend samples," *Rock Mechanics and Rock Engineering*, vol. 50, no. 1, pp. 17–28, 2017.

[19] Y. Wang, X. Hu, L. Liang, and W. Zhu, "Determination of tensile strength and fracture toughness of concrete using notched 3-p-b specimens," *Engineering Fracture Mechanics*, vol. 160, pp. 67–77, 2016.

[20] ASTM C78/C78M-18, *Standard Test Method for Flexural Strength of Concrete (Using Simple Beam with Third-Point Loading)*, ASTM International, West Conshohocken, PA, USA, 2018.

[21] Ł. Skarżyński, M. Nitka, and J. Tejchman, "Modelling of concrete fracture at aggregate level using FEM and DEM based on X-ray μCT images of internal structure," *Engineering Fracture Mechanics*, vol. 147, no. 10, pp. 13–35, 2015.

[22] A. Hillerborg, "Application of the fictitious crack model to different types of materials," *Current Trends in Concrete Fracture Research*, vol. 51, no. 2, pp. 95–102, 1991.

[23] J. P. Zuo, N. Chai, and H. W. Zhou, "Investigation on failure behaviour of basalt from different depths based on three-point bending meso-experiments," *Chinese Journal of Rock Mechanics and Engineering*, vol. 32, no. 4, pp. 689–695, 2013.

[24] Q. F. Guo, X. Wu, M. F. Cai, X. Xi, and F. H. Ren, "Strength characteristics and failure mode test of prefabricated fractured granite," *Journal of Engineering Science*, vol. 41, no. 1, pp. 43–52, 2019.

[25] X. Z. Hu and K. Duan, "Size effect and quasi-brittle fracture: the role of FPZ," *International Journal of Fracture*, vol. 154, no. 1-2, pp. 3–14, 2009.

[26] Z. P. Bazant and W. F. Schell, "Fatigue fracture of high-strength concrete and size effect," *ACI Materials Journal*, vol. 90, no. 5, p. 472, 1993.

[27] J. P. Zuo, Y. M. Huang, and L. F. Liu, "Investigation on meso-fracture mechanism of basalt with offset notch based on in-situ three-point bending tests," *Chinese Journal of Rock Mechanics and Engineering*, vol. 32, no. 4, pp. 740–746, 2013.

[28] Y. Miao, C. W. Zhu, Y. J. Yu, and Q. L. Yu, "Numerical simulation for calculating the tensile strength and fracture toughness based on different grain sizes," *Journal of Northeast University (Natural Science Edition)*, vol. 38, no. 6, pp. 864–868, 2017.

[29] X. Hu and K. Duan, "Size effect: influence of proximity of fracture process zone to specimen boundary," *Engineering Fracture Mechanics*, vol. 74, no. 7, pp. 1093–1100, 2007.

[30] J. Wei, W. C. Zhu, and R. Li, "Three-point bending test study on rock tensile strength and fracture toughness," *Journal of Water Resource and Architectural Engineering*, vol. 14, no. 3, pp. 128–132, 2016.